THE JOURNAL OF BIOLOGICAL CHEMISTRY
Vol. 276, No. 11, Issue of March 16, pp. 7727–7733, 2001

Printed in U.S.A.

Human 5-Aminoimidazole-4-carboxamide Ribonucleotide Transformylase/Inosine 5′-Monophosphate Cyclohydrolase

A BIFUNCTIONAL PROTEIN REQUIRING DIMERIZATION FOR TRANSFORMYLASE ACTIVITY BUT NOT FOR CYCLOHYDROLASE ACTIVITY*

Received for publication, October 31, 2000, and in revised form, November 20, 2000
Published, JBC Papers in Press, November 28, 2000, DOI 10.1074/jbc.M009940200

James M. Vergis‡, Karen G. Bulock§, Karen G. Fleming¶, and G. Peter Beardsley§‖**

From the ‡Department of Molecular Biophysics and Biochemistry, Yale University, New Haven, Connecticut 06520, the Departments of §Pharmacology and ‖Pediatrics, Yale University School of Medicine, New Haven, Connecticut 06510, and the ¶Department of Biophysics, The Johns Hopkins University, Baltimore, Maryland 21218

The bifunctional enzyme aminoimidazole carboxamide ribonucleotide transformylase/inosine monophosphate cyclohydrolase (ATIC) is responsible for catalysis of the last two steps in the *de novo* purine pathway. Gel filtration studies performed on human enzyme suggested that this enzyme is monomeric in solution. However, cross-linking studies performed on both yeast and avian ATIC indicated that this enzyme might be dimeric. To determine the oligomeric state of this protein in solution, we carried out sedimentation equilibrium analysis of ATIC over a broad concentration range. We find that ATIC participates in a monomer/dimer equilibrium with a dissociation constant of 240 ± 50 nM at 4 °C. To determine whether the presence of substrates affects the monomer/dimer equilibrium, further ultracentrifugation studies were performed. These showed that the equilibrium is only significantly shifted in the presence of both AICAR and a folate analog, resulting in a 10-fold reduction in the dissociation constant. The enzyme concentration dependence on each of the catalytic activities was studied in steady state kinetic experiments. These indicated that the transformylase activity requires dimerization whereas the cyclohydrolase activity only slightly prefers the dimeric form over the monomeric form.

Aminoimidazole carboxamide ribonucleotide transformylase/inosine monophosphate cyclohydrolase (ATIC)[1] is a bifunctional enzyme catalyzing the last two steps in the *de novo* purine biosynthetic nucleotide pathway (Fig. 1). The penultimate step, 5-aminoimidazole-4-carboxamide ribonucleotide transformylase (AICAR TFase), involves the transfer of the formyl group from a reduced folate substrate, (6R)N^{10}-formyltetrahydrofolate (10-f-FH_4), to the exocyclic amino group of AICAR to form 5-formylaminoimidazole-4-carboxamide ribonucleotide (FAICAR). The final step in the pathway, inosine monophosphate cyclohydrolase (IMPCHase), is a ring closure reaction of FAICAR forming inosine 5′-monophosphate (IMP) and a molecule of water.

Interest in ATIC partly comes from the fact that it is a potential chemotherapeutic target. AICAR TFase, along with the third enzymatic activity in the pathway, glycinamide ribonucleotide transformylase (TFase), utilizes the same reduced folate substrate making these two enzymes potential targets for anti-folate drugs. The anti-folate (6S/R)5,10-dideaza-5,6,7,8,-tetrahydrofolate (DDATHF) has been shown to be a potent antiproliferative agent, blocking *de novo* purine synthesis by inhibition of glycinamide ribonucleotide TFase and possibly AICAR TFase (1–4). Inhibition of AICAR TFase by metabolites of the folate analog methotrexate has been implicated in the mechanism of controlling inflammation due to arthritis and other inflammatory diseases (5–7).

The human form of ATIC (hATIC) was first cloned in our laboratory from a hepatoma cDNA library (8). Sugita *et al*. (9) later found an additional form of hATIC cloned from a human placenta cDNA library. This isoform differs from our original form in the six N-terminal amino acids, as well as in a substitution of glycine for aspartate at position 165 (9). We will refer to these isoforms as hATIC-a and hATIC-b, respectively. Because results from Sugita *et al*. (9) suggest that hATIC-b is more prevalent in human cells, this isoform of hATIC was used in all experiments described here.

Previously reported experiments attempting to determine the oligomeric state of ATIC have yielded contradictory results. Enzyme cross-linking experiments using both yeast isoforms and the avian form of the enzyme suggest that ATIC may form a dimer (10, 11). Gel filtration experiments using recombinant human enzyme conducted by Rayl *et al*. (8) suggested that ATIC exists as a monomer under the conditions tested (8). These apparently conflicting conclusions may actually both be valid, because the results depend greatly on the experimental conditions used to study the oligomeric properties of a protein. The questions of whether ATIC exists as a monomer or some other higher oligomeric species and which oligomeric form of the enzyme is the active species need to be addressed because of their importance for further understanding the structure-function relationships of this enzyme. This information will be critically important for postulating catalytic mechanisms for each activity and in the structure-based rational design of inhibitors targeting this enzyme.

* This work was supported in part by National Institutes of Health Grants R01CA50721 (to G. P. B.), GM16769 (to K. G. F.), and GM51245 (to Donald M. Engelman). The costs of publication of this article were defrayed in part by the payment of page charges. This article must therefore be hereby marked "*advertisement*" in accordance with 18 U.S.C. Section 1734 solely to indicate this fact.

** To whom correspondence should be addressed: Dept. of Pediatrics, Yale University School of Medicine, LMP 3096, 333 Cedar St., New Haven, CT 06510. Tel.: 203-785-4640; Fax: 203-737-2228; E-mail: g.beardsley@yale.edu.

[1] The abbreviations used are: ATIC, aminoimidazole ribonucleotide transformylase/inosine monophosphate cyclohydrolase; 10-f-FH_4, (6R)N^{10}-formyltetrahydrofolate; AICAR, 5-aminoimidazole-4-carboxamide ribonucleotide; TFase, transformylase; CV, column volumes; DDATHF, (6S/R)5,10-dideaza-5,6,7,8,-tetrahydrofolate; FAICAR, 5-formylaminoimidazole-4-carboxamide ribonucleotide; hATIC, human ATIC; IMP, inosine 5′-monophosphate; IMPCHase, inosine monophosphate cyclohydrolase; PCR, polymerase chain reaction.

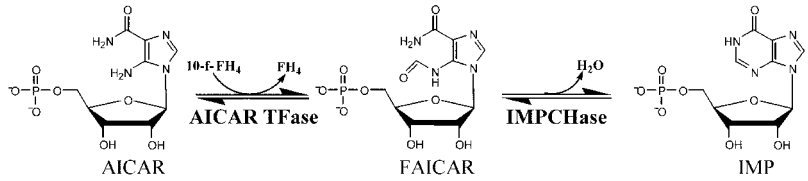

FIG. 1. **Reactions catalyzed by the AICAR TFase and IMPCHase activities of ATIC.**

In this report we demonstrate that ATIC exists in a monomer/dimer equilibrium and that this equilibrium is perturbed when both a folate analog and AICAR substrate are present but is not significantly shifted when each substrate is added individually. Evidence in support of these conclusions comes primarily from sedimentation equilibrium analytical ultracentrifugation studies of hATIC with and without substrate. We also show that for the IMPCHase enzymatic activity, both oligomeric forms possess catalytic activity with the dimeric form being more active. For the AICAR TFase enzymatic activity, the dimer appears to be the active form with the monomer possessing little or no catalytic activity.

EXPERIMENTAL PROCEDURES

Cloning of hATIC-b Expression Vector from hATIC-a—To clone the hATIC-b isoform of hATIC, PCR was used to change the first six amino acids, as well as the glycine at position 164, in the original clone hATIC-a using pETHATNB-1800 (8) as the initial PCR template. The primers used in the initial PCR reaction to change the first six amino acids were as follows: ATIC-a/b sense, 5′-GAGTTAAGCTAGCATG-**GCTCCCGGCCAGCTCGCC**TTATTTAGTGTCTCTGAC and ATIC antisense, 5′-CCCATGGATCCTCAGTGGTGGAAGAGCCGAAGGTTC. Unique *Nhe*I and *Bam*HI sites are *underlined*, and the sequence changes are indicated in *bold*. The PCR product was resolved on a 1% agarose gel, purified using the QIAquick gel extraction kit (Qiagen), and double-digested with *Nhe*I and *Bam*HI (New England BioLabs, Inc.). The resulting fragment was directionally cloned into the *Nhe*I and *Bam*HI polylinker sites of expression vector pET28a(+) (Novagen, Inc.) using T4 DNA ligase (New England BioLabs, Inc.). Selection of these restriction sites incorporated an N-terminal histidine·tag onto the clone to facilitate purification. This new clone was named pEThybrid-a/b.

Site-directed mutagenesis of G165D[2] using the method of overlap extension (12) was then carried out using pEThybrid-a/b as the template. Two PCR reactions were carried out using the following primers: ATIC-b sense, 5′-GAGTTAAGCTAGCATGGCTCCCGGCCAGCTC and G165D reverse, 5′-CTCCAAGGAGGT**GTC**CTTACTCTCGGAGC in the first reaction, and G165D forward, 5′-CTCCGAGAGTAAG**GAC**AC-CTCCTTGGAG and ATIC antisense (shown above) in the second reaction. The *Nhe*I site is *underlined* in the ATIC-b sense primer, and the G165D mutation is indicated in *bold*. These PCR products were resolved on a 1% agarose gel and purified as above. These products were then used in a second PCR reaction acting as both primer and template along with the ATIC-b sense and ATIC antisense primers to generate the full-length ATIC-b cDNA containing *Nhe*I and *Bam*HI restriction sites. This product was inserted into pET28a(+) as described above creating plasmid pETATIC-b. The sequence of this new clone was verified by automated sequencing at the Howard Hughes Medical Institute Biopolymer/W. M. Keck Foundation Biotechnology Resource Laboratory at Yale University.

Human ATIC Expression and Purification—Plasmid pETATIC-b was transformed into *Escherichia coli* Tuner™(DE3) (Novagen, Inc.) by heat shock. *E. coli* transformants were grown in 2YT bacterial media (13) with 50 μg/ml kanamycin (International Biotechnologies, Inc.) at 37 °C to an A_{600} value between 0.6 and 0.8. These cultures were then induced with 400 μM isopropyl-β-D-thiogalactopyranoside (American Bioanalytical) and grown at 30 °C for 3 h. The cells were harvested by centrifugation, washed with cold 0.85% NaCl, and either used immediately or stored at −80 °C.

Cell pellets were dissolved in cold lysis buffer (20 mM NaH_2PO_4, pH 8.0, and 100 mM NaCl). The cell suspension was lysed by sonication on a Fisher sonic dismembraner, model 300. The lysate was cleared by ultracentrifugation at 4 °C, 15,000 × *g* for 30 min in a Beckman Ti45 rotor. The supernatant solution containing soluble ATIC protein was poured off and placed on ice.

The immobilized metal affinity chromatography purification was performed on a BioCAD® Sprint chromatography work station (PerkinElmer Life Sciences) using a column containing POROS metal chelate media (PerkinElmer Life Sciences). The column was charged with 5 column volumes (CV) of 0.1 M $NiSO_4 \cdot 6H_2O$, washed with 10 CV of water, and equilibrated with 10 CV of 99.9% lysis buffer and 0.1% elution buffer (20 mM NaH_2PO_4, pH 8.0, 100 mM NaCl, 250 mM imidazole). The column was then loaded with 10–20 ml of cell lysate, washed with 99.9% lysis buffer and 0.1% elution buffer for 5 CV, and gradient-washed for 20 CV starting with 99.9% lysis buffer and 0.1% elution buffer and ending with 80.0% lysis buffer and 20.0% elution buffer. ATIC was eluted with 5 CV of 100% elution buffer collecting 2-ml fractions. The flow rate was 10 ml/min throughout the purification. Fractions were then assayed for either IMPCHase or AICAR TFase activity as described below. Those fractions containing activity were pooled and concentrated to 10–15 ml using a 250-ml Amicon ultrafiltration cell with a Diaflo YM30 ultrafiltration membrane (Amicon, Inc.). The protein solution was loaded onto a HiLoad 16/60 Superdex 200-pg gel filtration column (Amersham Pharmacia Biotech) equilibrated and washed with HB buffer (20 mM Tris-Cl, pH 7.5, 150 mM NaCl, 50 mM KCl, 5 mM EDTA, 5 mM dithiothreitol) at a rate of 1 ml/min for 150 ml on a fast performance liquid chromatography system (Amersham Pharmacia Biotech). Fractions (1 ml) containing activity were pooled and stored at 4 °C in HB buffer until needed.

Enzyme Activity Assays—All enzyme activity assays were performed on a PerkinElmer Life Sciences UV-visible Lambda2 spectrophotometer with PECSS data acquisition software unless noted otherwise. All reaction mixtures were 500 μl in volume and performed in a 1-cm pathlength quartz cuvette at room temperature unless noted otherwise.

AICAR TFase activity was followed by monitoring the formation of tetrahydrofolate at A_{298} based on a previously reported method (11, 14). Each reaction mixture contained a final concentration of 66 mM Tris-Cl, pH 7.4, 100 μM 10-f-FH_4, 50 μM AICAR, and 50 mM KCl unless noted otherwise. Each assay was initiated by rapid mixing of the substrates with the assay solution in the cuvette. The 10-f-FH_4 was synthesized as described previously (8, 15, 16) from (6S)5-formyl-5,6,7,8-tetrahydrofolic acid (leucovorin) purchased from Schircks Laboratories. AICAR was purchased from Sigma.

IMPCHase activity was followed by monitoring the formation of IMP at A_{248} based on a previously reported method (11). Each reaction mixture contained a final concentration of 100 mM Tris-Cl, pH 7.4, and 0.1 mM FAICAR unless noted otherwise. Each assay was initiated by rapid mixing of the substrate with the assay solution in the cuvette. FAICAR with synthesized from AICAR (Sigma) according to previously published procedures (11, 17).

Sedimentation Equilibrium of hATIC-b—A Beckman Optima™ XL-I ultracentrifuge was used to determine the equilibrium distribution of hATIC-b in HB buffer using the Rayleigh interference optics to visualize the protein. The interference experiments were carried out using external loading two-sector cells with sapphire windows. Data were collected at 4 °C at three initial concentrations of 3.5, 8.7, and 10.7 μM for hATIC-b at rotor speeds of 10,800, 13,300, and 16,000 rpm. For all experiments, water-water blanks were obtained at each speed prior to running the solutions of interest without disassembly of the cells between runs. Both the sample and buffer volumes were 125 μl.

The effect of substrates/inhibitors upon the equilibrium distribution was also investigated. The hATIC-b samples contained 200 μM AICAR with 2.1 and 9.1 μM enzyme, 1 mM 10-f-FH_4 with 2.7 and 5.1 μM enzyme, or both 200 μM AICAR and 500 μM DDATHF (18) with 3.7 and 7.6 μM enzyme. Substrates were added to the enzyme samples by dialysis using Pierce Slide-A-Lyzer® mini dialysis units. Data were collected at rotor speeds of 13,300, 16,000, and 18,500 rpm.

The program WinReedit[3] was used to select the ranges of data for further analysis and to correct for all sets of fringe displacements by

[2] Because of an additional amino acid in the N terminus of hATIC-b, the glycine to aspartate difference is at position 165 in hATIC-b and at position 164 in hATIC-a.

[3] WinReedit and WinMatch were written by J. W. Lary and D. A. Yphantis and are available on the Reversible Associations in Structural and Molecular Biology anonymous FTP site on the Internet.

subtracting the water-water blanks from the interference data. The attainment of sedimentation equilibrium was verified using the program WinMatch.[3] Equilibrium was usually established in 30–36 h. The equilibrium distributions were then analyzed using Winnl106[4] (19) by performing a global fit of all the data sets to obtain estimates for the association states and equilibrium constants. The program Sednterp,[5] which is based on the method of Laue (20), was used to calculate the protein partial specific volume from the amino acid composition of hATIC-b. This value was calculated to be 0.7304 ml/g at 4 °C. Sednterp also calculated the solvent density to be 1.01004 g/ml at 4 °C and the monomer molecular mass of ATIC-b to be 67,314. Data in fringe units were converted to molar concentrations using the constant 3.33 fringes·mg^{-1}·ml^{-1} protein and the predicted monomer molecular mass.

Equilibrium Concentration Dependence Assays—Using the determined dissociation constant from the sedimentation equilibrium analytical ultracentrifugation experiments, enzyme stock assay solutions ranging from 8.6 nM to 4.3 μM and spanning the percent dimer distribution curve from 6 to 77% were made. Initial stock solutions of hATIC-b were diluted to obtain the final concentration in each assay solution. The concentrations of these initial stocks were determined using Pierce Coomassie® Plus protein assay reagent with bovine serum albumin as a standard. Each assay solution contained 66 mM Tris-Cl, pH 7.4, 50 mM KCl, and enzyme. The solutions were allowed to reach their oligomeric equilibrium for at least 48 h at 4 °C in the cold room. The next day, separate assays for AICAR TFase and IMPCHase activity were performed at 4 °C as described above using a 0.1-cm pathlength quartz cuvette. The reaction volume of each assay was 200 μl with the final concentrations of each of the substrates, 10-f-FH_4 and AICAR for the AICAR TFase assay and FAICAR for the IMPCHase assay, at 0.5 mM. All assay and substrate solutions were kept at a constant temperature in the cold room before being assayed. Reactions were initiated by the rapid mixing of substrate and assay solution in the cuvette.

Pre-steady State Burst Experiments—The rapid quench experiments were carried out at 37 °C using a KinTek RFQ-3 rapid chemical quench apparatus (KinTek Instruments, State College, PA). Reactions were initiated by mixing 15 μl of enzyme with 15 μl of substrate solution containing [^{3}H]AICAR (10–20 Ci/mmol; Moravek Biochemicals) and 10-f-FH_4. The reaction buffer contained 50 mM triethylammonium bicarbonate, pH 8.0, 25 mM KCl, and 5 mM β-mercaptoethanol. The concentrations of enzyme and substrates cited in the text are those after mixing and during the reaction. Reactions were terminated by quenching with 67 μl of triethylamine (Sigma) and collected in 1.5-ml tubes containing 70 μl of chloroform (J. T. Baker, Inc.). Tubes were immediately vortexed and kept on ice until all of the samples in the set were collected. Samples were then centrifuged at 4000 × *g* for 10 min to separate the aqueous and organic phases. The aqueous phase was transferred to a clean tube, lyophilized, and redissolved in 8 μl of water for subsequent TLC separation on POLYGRAM® CEL 300 polyethyleneimine/UV_{254} TLC plates (Macherey-Nagel, GmbH & Co. Kg). TLC separation of substrates and products was carried out by slight modification of the method described previously (21).

Pre-steady state burst experiments were fit using the curve-fitting program, KaleidaGraph (Synergy Software), to the burst equation,

$$y = A(1 - e^{-kt}) + Ak_{SS}t \quad \text{(Eq. 1)}$$

where A = amplitude of the burst phase, k = observed burst rate, k_{ss} = steady state or linear phase rate, and t = time.

RESULTS

Human ATIC Exists in a Monomer/Dimer Equilibrium—Sedimentation equilibrium analytical ultracentrifugation was used to examine the oligomeric structure of hATIC in solution. A global nonlinear least squares analysis using Winnl106 was carried out on nine data sets obtained from three initial protein concentrations and three rotor speeds. The residuals of the fitting trials suggest that the simplest model that adequately describes the data contains three species with molecular weights corresponding to an ATIC monomer, dimer, and trimer. The formal expression is as follows:

$$c_i = c_{ref}\exp[\sigma(\xi_i - \xi_{ref})] + c_{ref}^2 K_{1,2}\exp[2\sigma(\xi_i - \xi_{ref})] + c_{ref,nmer}\exp[n\sigma(\xi_i - \xi_{ref})] + base \text{ where } \sigma = \frac{M(1-\bar{\nu}\rho)\omega^2}{2RT} \quad \text{(Eq. 2)}$$

where c_i is the total fringe displacement at a radial position, r_i, c_{ref} is the fringe displacement at a reference position r_{ref}, M is the monomer molecular mass, $\bar{\nu}$ is the monomer partial specific volume, ρ is the solvent density, ω is the angular velocity (radians·sec^{-1}), R is r_i, the universal gas constant, T is the absolute temperature, $\xi = r^2/2$, $K_{1,2}$ is the apparent monomer/dimer equilibrium constant (in fringe units) that was common for all data sets, and *base* is a baseline term for nonsedimentating material.

A typical distribution at 13,300 rpm is shown in Fig. 2. The fit was judged to be good by examination of the residuals (small and random) and minimization of the variance (1.13×10^{-2} with 2397 degrees of freedom). From this global fit, the dimer/

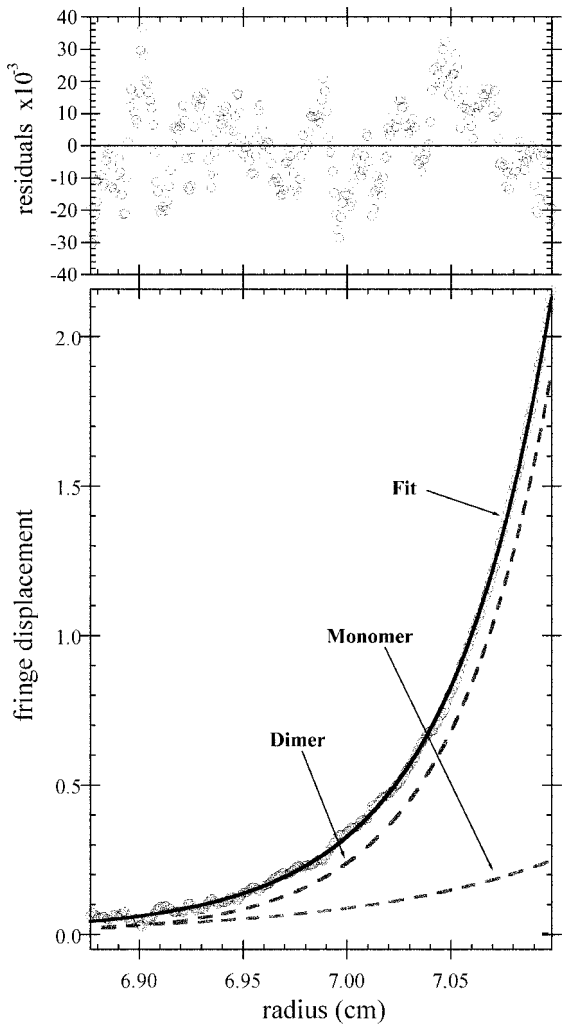

FIG. 2. **Sedimentation equilibrium distribution of 8.7 μM human ATIC at 13,000 rpm, 4 °C.** The *circles* in the *lower panels* are the data points, and the *solid lines* represent the best fit described by global analysis of all nine data sets to a monomer/dimer nonequilibrating trimer model although no trimer was observed in this particular data set. The individual exponents are labeled accordingly. The residuals of the fit are shown in the *upper panel* as *circles*.

[4] Winnl106 was written by M. L. Johnson, J. W. Lary, and D. A. Yphantis and is available on the Reversible Associations in Structural and Molecular Biology anonymous FTP site on the Internet.

[5] Sednterp was written by D. T. Hayes, T. M. Laue, and J. Philo and is available on the Reversible Associations in Structural and Molecular Biology anonymous FTP site on the Internet.

TABLE I

Effect of substrates on the dissociation constant for hATIC

Centrifuge data were measured as described under "Experimental Procedures" for each of the conditions below. The estimated dissociation constants for each of the substrate conditions are summarized below, along with the variance from each of the global fits. All data were globally fit using Equation 2, with a monomer/dimer equilibrium with some nonequilibrating trimer.

Condition tested	K_d (nM)	Square root of the variance
hATIC alone	240 ± 50	1.13×10^{-2} with 2397 degrees of freedom
+ AICAR	160 ± 30	9.64×10^{-3} with 1791 degrees of freedom
+ 10-f-FH_4	150 ± 30	8.63×10^{-3} with 1761 degrees of freedom
+ DDATHF and AICAR	31 ± 9	9.82×10^{-3} with 1686 degrees of freedom

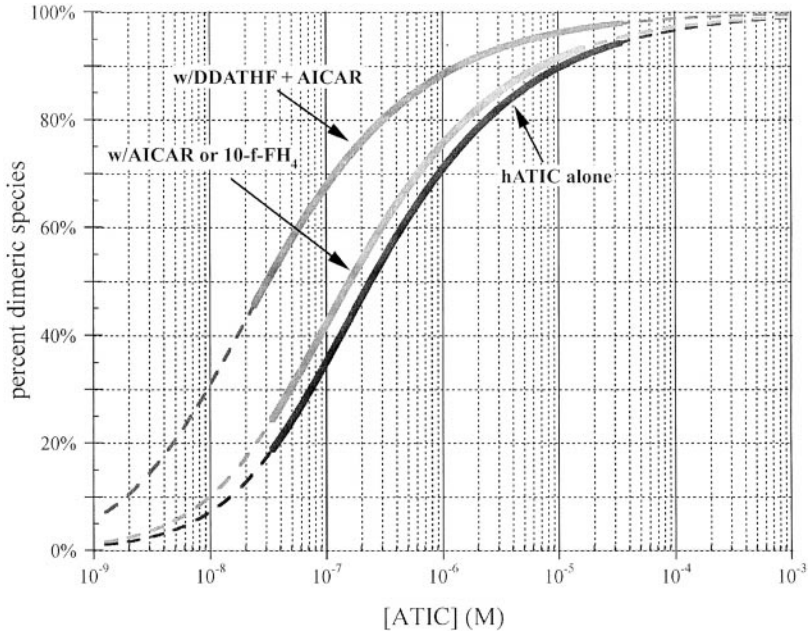

FIG. 3. **Effect of substrates on the percent dimer species distribution.** The distribution of the dimeric species was calculated as a function of total molar concentration of hATIC from their respective estimated equilibrium constants at 4 °C. The conditions for each distribution are labeled in the *figure*. The *solid* portions of the *curves* represent the concentration range in which the equilibrium analysis was carried out. The *dotted* portions of the *curves* are extrapolations of those data.

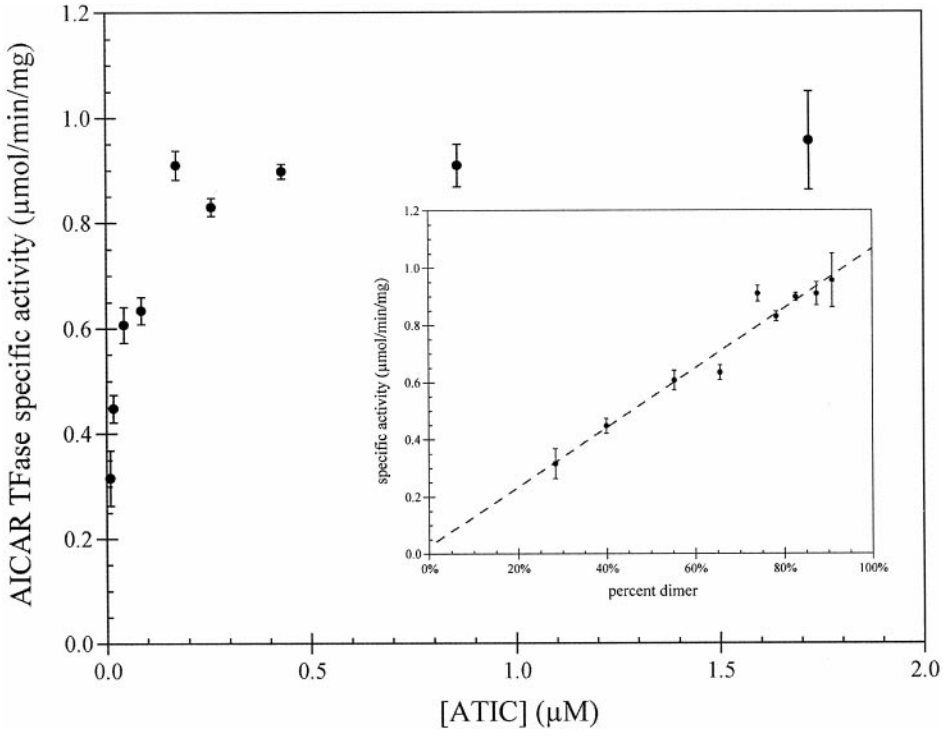

FIG. 4. **Effect of human ATIC concentration on the AICAR TFase activity.** A small volume of concentrated substrate solution containing AICAR (500 μM) and 10-f-FH_4 (500 μM) was combined with a solution containing the given concentration of human ATIC at its oligomeric equilibrium. Upon mixing, the reaction was followed by monitoring the A_{298}. The specific activity of the AICAR TFase reaction was plotted against ATIC concentration. *Inset*, the specific activities were plotted against the percent dimeric ATIC based upon the estimated dissociation constant for ATIC in the presence of AICAR and DDATHF. The *dotted line* is a linear fit of the data (r = 0.9769). The errors are the S.D. of the specific activities from the raw data.

monomer dissociation constant was estimated to be 240 ± 50 nM at 4 °C using Equation 2. Attempts to globally fit the data using a fitting function containing a common monomer-trimer dissociation constant for all data sets failed to converge as indicated by nonrandomness of the residuals and significant increase in the variance (data not shown). The global analysis thus suggests that the trimer does not reversibly associate with the other species on the time scale of this experiment and is considered thermodynamically heterogeneous.

Effect of Substrates on the Dimerization of ATIC—The obser-

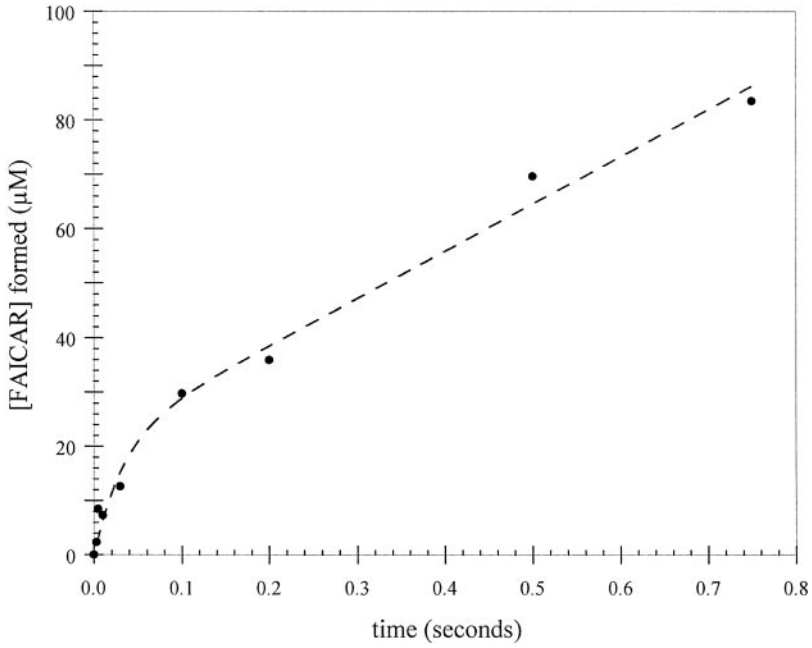

FIG. 5. **Kinetics of pre-steady state burst in the AICAR TFase reaction.** A solution of hATIC was mixed with a solution of [^{3}H]AICAR and 10-f-FH_4 to give final concentrations of hATIC (20 μM), AICAR (100 μM), and 10-f-FH_4 (500 μM). The formation of [^{3}H]FAICAR was monitored. The *circles* represent the data points observed, and the *dotted line* represents the data fit to the burst equation (r = 0.9950).

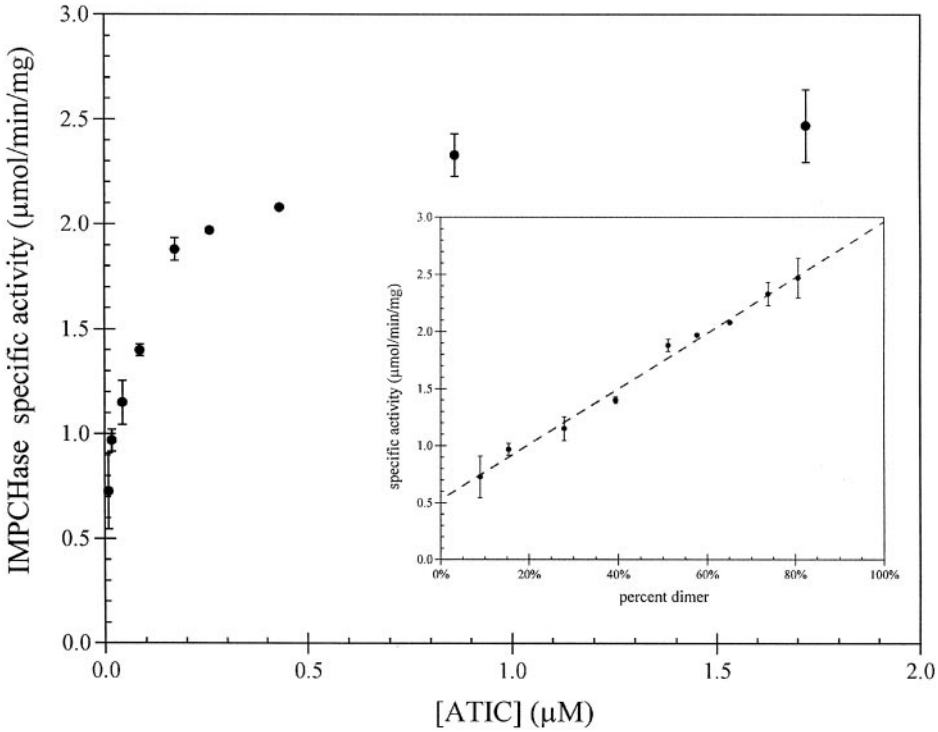

FIG. 6. **Effect of human ATIC concentration on the IMPCHase activity.** A small volume of concentrated substrate solution containing FAICAR (500 μM) was combined with a solution containing the given concentration of human ATIC at its oligomeric equilibrium. Upon mixing, the reaction was followed by monitoring the A_{248}. The specific activity of the IMPCHase reaction was plotted against ATIC concentration. *Inset*, the specific activities were plotted against the percent dimeric ATIC based upon the estimated dissociation constant for ATIC in the presence of AICAR. The *dotted line* represents a linear fit of the data (r = 0.9952). The errors are the S.D. of the specific activities calculated from the raw data.

vation of a monomer/dimer equilibrium in this concentration range raises the possibility that the presence of substrates may affect the activity of ATIC by affecting the monomer/dimer equilibrium. Thus it is important to determine how the substrates influence the oligomeric state and which oligomeric form of ATIC is active for both the AICAR TFase and IMPCHase activities. To determine whether the monomer/dimer equilibrium of ATIC is shifted in the presence of one or more of its substrates, the sedimentation equilibrium experiments were repeated with solutions containing AICAR, 10-f-FH_4, or AICAR and the folate analog DDATHF at concentrations 10 times the K_m or the K_i in the case of DDATHF (4, 7, 8, 11, 21). A global nonlinear analysis was carried out as above using two initial concentrations at three rotor speeds for each of the above conditions using Winnl106. The simplest model that fit all the data sets for each condition tested contained three species corresponding to ATIC monomer, dimer, and some heterogeneous trimeric species as before. The results of these studies and their fit statistics are summarized in Table I. As seen in Fig. 3, in the presence of AICAR or 10-f-FH_4, the percent dimeric species is not significantly shifted from that of apo-hATIC. However, when both AICAR and the folate analog DDATHF are present, there is a considerable shift toward higher percent dimer in the molar species plot showing a relationship between the substrates and the oligomeric state of hATIC.

AICAR TFase Is Active as the ATIC Dimer—Knowing that the oligomeric equilibrium is affected by the presence of both AICAR and DDATHF, the concentration dependence of ATIC was investigated to determine whether the amount of dimeric protein has a correlation to the AICAR TFase activity. To study

this, steady state assays were performed within a concentration range of protein based upon the percent dimer curve in Fig. 3. The AICAR and 10-f-FH_4 substrates were concentrated so that the addition of the substrate mixture to the assay solution would not change the total volume by more than 5%. The concentration of substrate used was greater than 100 times the highest enzyme concentration and kept constant throughout so that binding would not be a concern during the experiment. The results shown in Fig. 4 suggest that upon increasing enzyme concentration, the AICAR TFase activity also increases. Correcting the predicted percent dimer for the effect of DDATHF and AICAR on the dissociation constant resulted in a statistically better linear fit of the data ($r = 0.9769$) (Fig. 4, *inset*). Extrapolation of this linear fit to zero percent dimer predicted a specific activity of only 0.03 μmol·min^{-1}·mg^{-1}. This suggests that the monomeric form of ATIC is essentially inactive, especially when compared with the dimer's specific activity of 1.1 μmol·min^{-1}·mg^{-1} found by extrapolation to 100% dimer.

The result that the dimer is the active form of ATIC for AICAR TFase activity is further supported by the results of pre-steady state burst assays carried out at protein concentrations ranging from 20 to 100 μM corresponding to 92 to 97% dimer. Fig. 5 shows a typical pre-steady state AICAR TFase burst experiment using a final concentration of 20 μM ATIC carried out at 37 °C. A fit of these data using Equation 1 results in an amplitude of 20 μM, which suggests that 100% of the AICAR TFase catalytic sites are active at this enzyme concentration.

IMPCHase Is Active in Both the ATIC Monomer and Dimer—An analogous set of experiments for the IMPCHase activity were also carried out on hATIC. The substrate FAICAR was concentrated so that the addition of the substrate mixture to the assay solution would not change the total volume by more than 5%. The concentration of substrate used was greater than 100 times the highest enzyme concentration and kept constant throughout so that binding would not be a concern during the experiment. These results shown in Fig. 6 suggest that upon increasing enzyme concentration, the IMPCHase activity also increases. The percent dimeric ATIC assayed was then calculated using the estimated dissociation constant calculated in the presence of AICAR, because AICAR has been shown to be an inhibitor of IMPCHase activity (22) and may contribute to slightly increased dimerization by binding to ATIC. This correction yielded a slightly statistically better fit ($r = 0.9952$) than the linear fit using the dissociation constant from hATIC alone ($r = 0.9934$), but the data points in both cases were within the error limits of each other (data not shown). Extrapolation of the linear fit to 0% dimer indicates a residual specific activity of 0.53 μmol·min^{-1}·mg^{-1} suggesting that the monomeric form of ATIC still possesses IMPCHase activity (Fig. 6, *inset*). This value is about 6-fold less than the predicted specific activity of 3.0 μmol·min^{-1}·mg^{-1} for 100% dimeric ATIC. This suggests that the dimeric form is the more active form for the IMPCHase activity.

Determination of the Apparent Dissociation Constant Using Oligomeric Kinetic Data—Another method derived by Kurganov (23) exists to determine the dissociation constant of an enzyme based on kinetic data gathered on a range of protein concentrations. This analysis was carried out on the AICAR TFase kinetic data using the relationship of Kurganov (23) for the case when only the dimeric form of the enzyme is active. This relationship is shown below in Equation 3,

$$\frac{1}{a_{total}} = \frac{1}{a_{dimer}} + \frac{1}{\sqrt{2K_{1,2}a_{dimer}}} \times \frac{1}{\sqrt{C_0 a_{total}}} \quad \text{(Eq. 3)}$$

where a_{total} is the observed specific activity, a_{dimer} is the specific activity from the dimeric portion of the protein, $K_{1,2}$ is the apparent monomer/dimer association constant, and C_0 is the initial enzyme concentration (23). Graphing the data in the coordinates $(a_{total})^{-1}$ *versus* $(C_0 a_{total})^{-1/2}$ produced a linear trend with a linear correlation coefficient of 0.9950 for the linear regression fit (data not shown). Using the slope and intercept values from the fit, the values of a_{dimer} and $K_{1,2}$ were calculated to be 1.06 μmol/min/mg and 0.035 nM^{-1}, respectively. This value of $K_{1,2}$ gives an apparent dissociation constant of 28 nM, which is in agreement with the dissociation constant calculated from the centrifugation data of hATIC in the presence of AICAR and DDATHF. Attempts to analyze the IMPCHase kinetic data were unsuccessful because of the difficulty in gathering data over a large enough concentration range required to satisfy the conditions where both the monomer and dimer possess enzymatic activity (23).

DISCUSSION

Our interest in understanding the structure-function relationships for ATIC has led us to characterize the oligomeric state of human ATIC. Using sedimentation equilibrium analytical ultracentrifugation we have shown that human ATIC exists in a monomer/dimer equilibrium with an apparent dissociation constant of 240 ± 50 nM at 4 °C. The two enzyme cross-linking studies reported previously (10, 11) support this finding, because both groups observed dimeric ATIC and neither observed any higher order species.

The effect of substrates proved interesting in that neither AICAR nor 10-f-FH_4 alone significantly changed the apparent dissociation constant, but when AICAR was present along with DDATHF, a folate analog of 10-f-FH_4, the apparent dissociation constant was reduced 10-fold, resulting in tighter dimer formation. Thus it appears that although neither of the substrates alone provides further stabilization of the dimer, when present together, there is considerable additional stabilization. This suggests that these two substrates bind ATIC in such a manner as to either directly bridge the dimeric interface of the homodimer or to induce a conformational change to increase the interactions between the monomer subunits.

Recent crystallographic studies on both the avian and human forms of ATIC by the Wilson group at The Scripps Research Institute suggest that the former is probably the case. Their findings have shown that ATIC crystallizes as a homodimer and that the presumed substrate binding site for the AICAR TFase activity consists of residues from both monomeric units of ATIC. The IMPCHase substrate binding site is completely localized in one monomeric unit, away from the dimeric interface.[6] This led us to investigate whether there is a fundamental relationship between dimerization and catalytic activity for the AICAR TFase and IMPCHase reactions. As seen in Fig. 4, there is an enzyme concentration dependence on AICAR TFase activity of ATIC, such that extrapolation of the specific activity to 0% dimer predicts practically no residual AICAR TFase activity. The values for the percent dimer were calculated using the estimated dissociation constant found with both folate and AICAR present, because both substrates are required for catalysis. Thus it appears that the dimeric form of ATIC is strongly preferred for AICAR TFase activity. This finding correlates with the structural data mentioned above in that the binding sites for the AICAR and folate substrate appear to be at the dimer interface and made up of constituents from both monomer subunits. Also, the pre-steady state burst experiments on the AICAR TFase activity, which

[6] S. E. Greasley, P. Horton, G. P. Beardsley, J. Ramcharan, S. J. Benkovic, and I. A. Wilson, submitted for publication.

were carried out at concentrations where ATIC is mostly dimeric, showed 100% of the catalytic sites were active. If the dimeric form of ATIC were not an active form of the enzyme, this number would be expected to be much lower.

As a check of our results, we analyzed our AICAR TFase kinetic data using a method derived by Kurganov (23). This was important to show that the assumption of using the estimated dissociation constant as determined in the presence of both AICAR and DDATHF was justified when plotting the AICAR TFase kinetic data, as well as to substantiate the value of the monomer/dimer dissociation constant obtained from the sedimentation equilibrium studies. This was of particular significance, because the value of 31 ± 9 nM calculated from the analytical ultracentrifuge data was near the limit of this technique. Using the Kurganov method, the estimated dissociation constant was calculated to be 28 nM, well within the error calculated from the sedimentation equilibrium method for the condition when both AICAR and DDATHF were present.

An enzyme concentration dependence was also found for the IMPCHase specific activity (Fig. 6); in this case, however, both the monomer and dimeric forms of ATIC appear to possess activity, with the dimeric form being more active. This result also fits the structural data, because the IMPCHase substrate binding site is completely localized in the monomeric subunit as stated above. The fact that the IMPCHase activity was greater when ATIC was in the dimeric form may possibly be attributed to the dimeric form of ATIC keeping the IMPCHase active site in a more active conformation. Perhaps the IMPCHase activity is more active in the dimeric form than the monomeric form to help facilitate the conversion of FAICAR formed from the AICAR TFase reaction, because it is the dimeric form that is required to provide the FAICAR for catalysis to IMP at the IMPCHase site.

The linking of the AICAR TFase and IMPCHase activities on the same polypeptide raises the question of whether these two activities are kinetically coupled to one another through either substrate channeling or communication between the two catalytic domains. Szabados and Christopherson (24) observed a decrease in the formation of [^{3}H]IMP from [^{3}H]AICAR when exogenous unlabeled FAICAR was added to the bifunctional enzyme reaction and interpreted this as indicating that substrate channeling does not occur in ATIC (24). However, those experiments were not in themselves enough to completely justify that conclusion. A detailed transient-phase kinetic study of the AICAR TFase and IMPCHase activities of ATIC is currently underway in our laboratory to unequivocally answer the substrate channeling question. Communication between the two active sites also seems unlikely, because the construction of truncation mutants of ATIC resulted in two separate, fully active, functional domains containing AICAR TFase activity on the C-terminal end and IMPCHase activity on the N-terminal end (8). This is further supported by the fact that IMPCHase inhibitors have no effect on the AICAR TFase kinetics (25). Regardless of whether channeling occurs in ATIC, there is yet an advantage to having these two activities located on the same polypeptide. Recent studies by ourselves[7] and others (25) have independently shown that the AICAR TFase reaction favors the reverse direction. The tethering of these two activities puts the IMPCHase and the AICAR TFase domains in close proximity to one another. The decreased distance between these two activities should help draw the overall reaction in the forward reaction by allowing the AICAR TFase domain to provide an increased local concentration of the intermediate FAICAR to the IMPCHase domain for conversion to IMP. If these two activities were located on separate proteins, the efficiency of the system would be reduced because of the dilution effects of diffusion through solvent and also the possible conversion of FAICAR back to AICAR. Because it is the dimeric form of ATIC providing the FAICAR for the IMPCHase domain, a more active IMPCHase activity in the dimeric form would help to make the overall reaction more efficient.

In conclusion, these studies of human ATIC provide an insight into the structure-function relationships of this important bifunctional enzyme in the *de novo* purine biosynthetic pathway. The results presented here show that ATIC exists in a monomer/dimer equilibrium but that the dimeric form is required for AICAR TFase activity whereas the IMPCHase possesses catalytic activity in both the monomeric and dimeric forms with the dimeric form being more active. These findings will be of greatest importance in postulating a catalytic mechanism for both activities of ATIC, especially for the AICAR TFase reaction. Also, these results could possibly be used in the design of inhibitors that do not target the active sites of this protein but those that inhibit dimerization of ATIC and thus inhibit the AICAR TFase reaction.

Acknowledgment—We thank Dr. Ian Wilson and his group for providing information regarding the crystal structure of ATIC. We are also grateful to Dr. Karen Anderson, Dr. Patrick Fleming, and Mark Wilson for helpful discussions.

[7] K. G. Bulock, G. P. Beardsley, and K. S. Anderson, manuscript in preparation.

REFERENCES

1. Baldwin, S. W., Tse, A., Gossett, L. S., Taylor, E. C., Rosowsky, A., Shih, C., and Moran, R. G. (1991) *Biochemistry* **30,** 1997–2006
2. Beardsley, G. P., Taylor, E. C., Grindey, G. B., and Moran, R. G. (1986) in *Chemistry and Biology of Pteridines* (Cooper, B. A., and Whitehead, V. M., eds) pp. 953–957, Walter de Gruyter & Co., New York
3. Beardsley, G. P., Moroson, B. A., Taylor, E. C., and Moran, R. G. (1989) *J. Biol. Chem.* **264,** 328–333
4. Beardsley, G., Pizzorno, G., Russello, O., Cashmore, A., Moroson, B., Cross, A., Wildman, D., and Grindey, G. (1990) in *Chemistry and Biology of Pteridines 1989. Pteridines and Folic Acid Derivatives* (Curtius, H.-C., Ghisla, S., and Blau, N., eds) pp. 1001–1008, Walter de Gruyter & Co., New York
5. Baggott, J. E., Vaughn, W. H., and Hudson, B. B. (1986) *Biochem. J.* **236,** 193–200
6. Cronstein, B. N., Naime, D., and Ostad, E. (1993) *J. Clin. Invest.* **92,** 2675–2682
7. Allegra, C. J., Drake, J. C., Jolivet, J., and Chabner, B. A. (1985) *Proc. Natl. Acad. Sci. U. S. A.* **82,** 4881–4885
8. Rayl, E. A., Moroson, B. A., and Beardsley, G. P. (1996) *J. Biol. Chem.* **271,** 2225–2233
9. Sugita, T., Aya, H., Ueno, M., Ishizuka, T., and Kawashima, K. (1997) *J. Biochem.* (*Tokyo*) **122,** 309–313
10. Tibbetts, A. S., and Appling, D. R. (2000) *J. Biol. Chem.* **275,** 20920–20927
11. Mueller, W. T., and Benkovic, S. J. (1981) *Biochemistry* **20,** 337–344
12. Ho, S. N., Hunt, H. D., Horton, R. M., Pullen, J. K., and Pease, L. R. (1989) *Gene* **77,** 51–59
13. Sambrook, J., Fritsch, E. F., and Maniatis, T. (1989) *Molecular Cloning: A Laboratory Manual*, 2nd Ed., Cold Spring Harbor Laboratory, Cold Spring Harbor, NY
14. Black, S. L., Black, M. J., and Mangum, J. H. (1978) *Anal. Biochem.* **90,** 397–401
15. Rabinowitz, J. C. (1963) *Methods Enzymol.* **6,** 814–815
16. Rowe, P. B. (1971) *Methods Enzymol.* **18,**733–735
17. Shaw, G., and Wilson, D. V. (1962) *J. Am. Chem. Soc.* 2937–2940
18. Taylor, E. C., Harrington, P. J., Fletcher, S. R., Beardsley, G. P., and Moran, R. G. (1985) *J. Med. Chem.* **28,** 914–921
19. Johnson, M. L., Correia, J. J., Yphantis, D. A., and Halvorson, H. R. (1981) *Biophys. J.* **36,** 575–588
20. Laue, T. M., Shah, B., Ridgeway, T. M., and Pelletier, S. L. (1992) in *Analytical Ultracentrifugation in Biochemistry and Polymer Science* (Harding, S. E., Rowe, A. J., and Horton, J. C., eds) pp. 90–125, Royal Society of Chemistry, Cambridge
21. Szabados, E., and Christopherson, R. I. (1994) *Anal. Biochem.* **221,** 401–404
22. Szabados, E., and Christopherson, R. I. (1998) *Int. J. Biochem. Cell Biol.* **30,** 933–942
23. Kurganov, B. I. (1967) *Mol. Biol.* (*Mosc.*) **1,** 17–27
24. Szabados, E., Wilson, P. K., and Christopherson, R. I. (1998) *Adv. Exp. Med. Biol.* **431,** 241–244
25. Wall, M., Shim, J. H., and Benkovic, S. J. (2000) *Biochemistry* **39,** 11303–11311